# Buoyancy driven miscible front dynamics in tilted tubes

T. Séon,[a] J.-P. Hulin,[b] and D. Salin
*Laboratoire Fluides Automatique et Systèmes Thermiques, UMR 7608, Bâtiment 502, Campus Universitaire, 91405 Orsay Cedex, France*

B. Perrin
*Laboratoire Pierre Aigrain, UMR 8551, Ecole Normale Supérieure, Département de Physique, 24 rue Lhomond, 75231 Paris Cedex, 05, France*

E. J. Hinch
*DAMTP-CMS, University of Cambridge, Wilberforce Road, CB3 OWA Cambridge, United Kingdom*

(Received 1 October 2004; accepted 6 January 2005; published online 22 February 2005)

The velocity $V_f$ of the fronts of light and heavy fluids in a tilted tube, interpenetrating many diameters, is studied as a function of the fluid viscosity $\mu$, Atwood number $\mathrm{At} \ll 1$ and tilt angle $\theta$ from vertical. Three flow regimes are observed: starting from vertical, $V_f$ first increases with $\theta$, reaches a plateau and then decreases again. In the first regime, $V_f$ is controlled by segregation and mixing effects, respectively, increasing and decreasing with $\theta$. On the plateau, $V_f$ is independent of the fluid viscosity and proportional to $(\mathrm{At}gd)^{1/2}$, indicating a balance between inertia and buoyancy. In the third regime close to horizontal, the fluids separate into two parallel countercurrents controlled by viscosity. The variations of $V_f$ with $\theta$, At, and $\mu$ in the second and third regimes and the crossover from one to the other are described by scaling laws based on characteristic viscous and inertial velocities. © *2005 American Institute of Physics*. [DOI: 10.1063/1.1863332]

Buoyancy induced interpenetration of miscible fluids of different densities due to the development of Rayleigh–Taylor like instabilities is a widespread phenomenon both in natural (ocean and atmosphere) and industrial systems. The present paper deals with such phenomena inside long tilted tubes as encountered both in chemical[1] and petroleum engineering (deviated wells). In contrast with many previous studies of the Rayleigh–Taylor instabilities,[2–5] we are interested in (i) late times when the mixing zone extends over tens of diameters, (ii) inclined tubes, (iii) small density contrasts (Boussinesq approximation), and (iv) moderate Reynolds numbers. More specifically, we measure the velocity $V_f$ of the penetration fronts as a function of the Atwood number $\mathrm{At}=(\rho_2-\rho_1)/(\rho_2+\rho_1)$, of the fluid viscosity $\mu$, and of the tilt angle $\theta$ with respect to vertical ($\rho_1$ and $\rho_2$ are, respectively, the densities of the light and the heavy fluid). The tilt $\theta$ plays a crucial role since the transverse gravity component present in tilted tubes induces a segregation of the two fluids inside the tube section: the lighter fluid moves preferentially towards the upper surface of the tube and the heavier fluid towards the lower one.

For immiscible fluids, a large amount of work[6–13] has been devoted to the related problem of the rise of large bubbles in vertical and tilted tubes, often in relation with applications to petroleum, nuclear and chemical engineering. In static vertical liquid columns of large diameter $d$, gas bubbles with a diameter of the order of $d$ and a length larger than $d$ were found by Davies and Taylor[6] to rise at a velocity $V_{Tb} \simeq 0.35 \times (gd)^{1/2}$. This value indicates a balance between inertial (Bernoulli-like) and buoyancy effects. For smaller tubes and/or viscous fluids, capillary and viscous effects modify the relation.[11,12]

For miscible fluids, these results are strongly modified through transverse mixing by shear induced instabilities of the interface between the fluids:[14] this reduces the local density contrasts and, therefore, buoyancy forces driving the front motion. In tilted tubes, the transverse gravity component reduces transverse mixing.[15] In our previous study,[16] longitudinal mixing along the tube was indeed observed to depend strongly on the tilt angle $\theta$. In the present paper we demonstrate that $\theta$ also influences considerably the front velocity and that, as $\theta$ increases, there is a transition from front velocities controlled by inertial forces towards viscosity controlled velocities.

The study is performed in a 4 m long transparent tube with an internal diameter $d=20$ mm that can be tilted to all angles between vertical and horizontal. The lighter fluid is water dyed with nigrosine (40 mg/l) and the heavy one is a solution of water and $CaCl_2$ salt: At varies from $4\times10^{-4}$ to $3.5\times10^{-2}$. The viscosities of the two fluids are equal and may be varied between 1 and $4\times10^{-3}$ Pa s by adding glycerol to both of them. Initially, the heavier and lighter fluids are, respectively, located in the upper and lower halves of the tube and separated by a gate valve. The tube is illuminated from behind and, after opening the valve, pictures are taken at regular intervals using a digital camera which provides spatiotemporal diagrams of the mean concentration profiles along the tube.[14] The displacement of the fronts with time is marked on these diagrams by sharp boundaries between domains of different relative concentrations of the fluids. The front velocity $V_f$ is equal to the slope of these boundaries: it becomes constant with time after a couple of diameters

[a]Electronic mail: seon@fast.u-psud.fr
[b]Author to whom correspondence should be addressed. Telephone: 33 1 69 15 80 62. Fax: 33 1 69 15 80 60. Electronic mail: hulin@fast.u-psud.fr

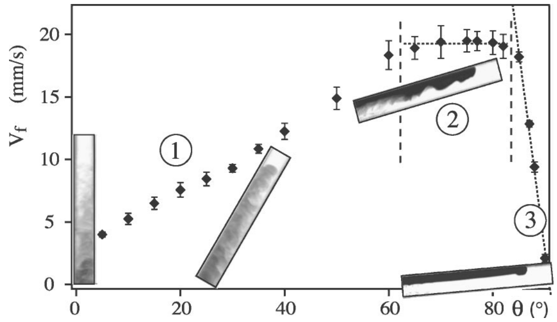


FIG. 1. Front velocity as a function of the tilt angle $\theta$ ($At=4\times10^{-3}$, $\mu=10^{-3}$ Pa s). The insets are pictures of a 30 cm long section of tube just above the gate valve in the corresponding flow domains. The dashed lines represent the boundaries between the domains and the dotted lines are only guides for the eye.

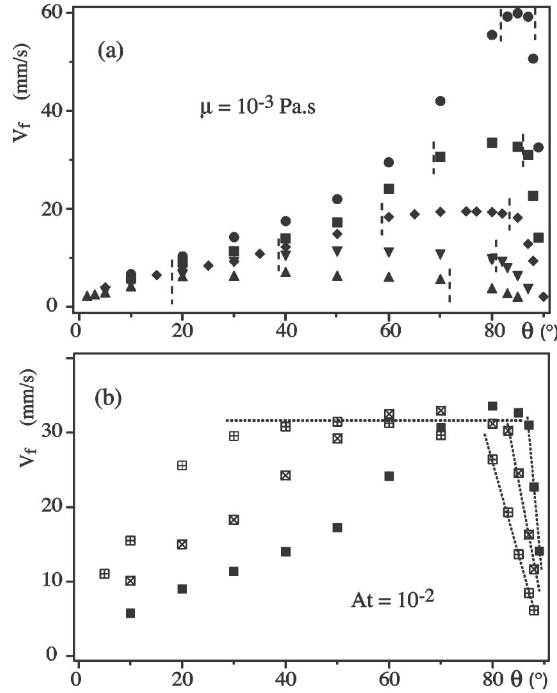


FIG. 2. Front velocity as a function of the tilt angle $\theta$ (a) for a constant viscosity ($\mu=10^{-3}$ Pa s) and different density contrasts $At=3.5\times10^{-2}$ (•), $10^{-2}$ (■), $4\times10^{-3}$ (◆), $10^{-3}$ (▼), $4\times10^{-4}$ (▲). (b) For the same density contrast ($At=10^{-2}$) and different viscosities $\mu=10^{-3}$ Pa s (■), $2\times10^{-3}$ Pa s (⊠), $4\times10^{-3}$ Pa s (⊞).

within experimental uncertainty and has nearly the same value for both fluids due to the symmetry resulting from the small difference in density. For vertical tubes ($\theta=0$), the location of the front can often not be determined because (particularly at large density contrasts) it is too fuzzy (see left inset in Fig. 1). Note also that none of the experiments reported here correspond to horizontal tubes ($\theta=\pi/2$) for which $V_f$ would vary with time.

Figure 1 displays the variation of the front velocity $V_f$ as a function of $\theta$ for constant density contrast and viscosity. Three different types of variations are observed as the angle $\theta$ increases: at small $\theta$ values (domain 1), $V_f$ increases strongly with $\theta$ (almost a factor of 10 between 5° and 65°). This effect suggest analogies with the Boycott effect, namely, with the enhancement of the sedimentation velocity of particles in a tilted tube with respect to a vertical one due to a similar transverse segregation.[17] The flow behind the front is weakly turbulent (see the inset) and transverse mixing is efficient: it homogenizes quickly the relative concentration of both fluids in the tube section even though segregation effects are visible close to the front. In this same range of angles, the longitudinal mean concentration profile follows a macroscopic diffusion law.[16] For $65° < \theta < 82°$ (domain 2), $V_f$ remains about constant at a maximum value $V_f^M$. In this range of tilt angles, segregation is strong and a thorough mixing across the flow section is not achieved. The mean concentration profile is also no longer diffusive.[16] Finally, for $\theta > 82°$ (domain 3), $V_f$ decreases sharply while there is practically no mixing between the fluids (see inset at the bottom right of Fig. 1). Note that, in domains 2 and 3, the flow takes the form of a gravity current.[18,19] The same three domains are observed at different Atwood numbers At and viscosities $\mu$ [Figs. 2(a) and 2(b)].

In domain 1, for a given tilt angle, $V_f$ increases markedly with $\mu$ [Fig. 2(b)] and much slower with At [Fig. 2(a)]. The dependence on $\mu$ is compatible with a $\mu^{3/4}$.

In domain 2, on the contrary, the *plateau* value $V_f^M$ is found to increase with At [Fig. 2(a)] while it is almost constant with $\mu$ [Fig. 2(b)]. This suggests that, in this latter domain, $V_f^M$ is determined by a balance between buoyancy pressure forces scaling as $\Delta\rho g d$ and inertial terms scaling as $(\rho_1+\rho_2)V^2$ ($\Delta\rho=\rho_2-\rho_1$). Equating the two terms leads to the characteristic velocity:

$$V_t = \sqrt{Atgd}. \tag{1}$$

This expression coincides dimensionally with the velocity $V_{Tb}$ of inertial Taylor bubbles[6] for which the parameter At can be taken equal to 1 for air and water. Using the characteristic velocity $V_t$, one can define a Reynolds number:

$$Re_t = \frac{V_t d}{\nu} = \frac{\sqrt{Atgd}\, d}{\nu}. \tag{2}$$

In the following, $Re_t$ will be used as a control parameter to compare experimental results obtained for different density contrasts and/or viscosities.

Normalizing $V_f$ by $V_t$ (Fig. 3) allows us to collapse all velocities in the plateau region onto a single value $V_f^M/V_t \simeq 0.7$ independent of At and $\mu$ so that

$$V_f^M = 0.7\sqrt{Atgd}. \tag{3}$$

While the values of $V_f/V_t$ in the plateau region coincide, one observes in Figs. 2(b) and 3 that the range of $\theta$ values corresponding to domains 2 and 3 becomes broader at higher $\mu$ and lower At values while, conversely, domain 1 becomes narrower.

The fact that the value of $V_f^M/V_t$ in domain 2 does not depend on $\theta$ can be related to the qualitatively similar behavior of large gas bubbles rising in tilted tubes.[7,9] In that case, the bubble velocity increases with the tilt angle and reaches a maximum before decreasing for near horizontal tubes: the small variation of $V_f$ with $\theta$ in the plateau region may reflect

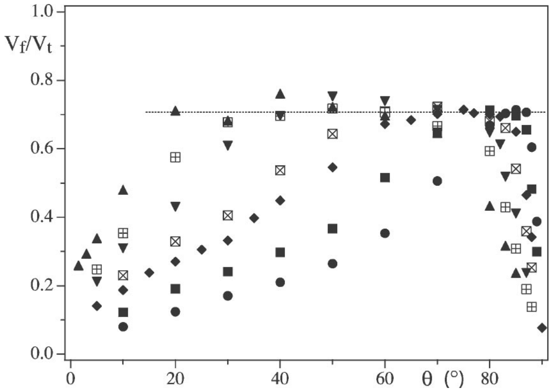


FIG. 3. Normalized front velocity $V_f/V_t$ variation with the tilt angle $\theta$ for different density contrasts and viscosities. Meanings of symbols are the same as in Figs. 2(a) and 2(b).

the vicinity of such a maximum. For horizontal tubes and inviscid fluids, Benjamin[18] found the same scaling law with a similar prefactor.

In domain 3, $V_f/V_t$ depends on $\mu$ for given $\theta$ and At values so that a second characteristic velocity $V_\nu$ needs to be defined. Visually, domain 3 corresponds to a quasiparallel counterflow of the two fluids. One can therefore consider dimensionally that, as for Poiseuille flow under gravity, the viscous force $\propto(\rho_1+\rho_2)\nu V/d^2$ is balanced by a buoyancy force $\Delta\rho g$. There results a characteristic "viscous" velocity:

$$V_\nu=\frac{\mathrm{At}gd^2}{\nu}. \tag{4}$$

Experimentally, the velocity expected in this regime is not $V_\nu$ but $V_\nu\cos\theta$. The additional factor $\cos\theta$ is due to the fact that the viscous counterflow is driven by the gravity component $\Delta\rho g\cos\theta$ parallel to the tube length and not by $\Delta\rho g$.

Assuming that $V_\nu\cos\theta$ is the proper scaling velocity in region 3, the variation of $V_f/(V_\nu\cos\theta)$ has been plotted in Fig. 4 as a function of the weighted Reynolds number $\mathrm{Re}_t\cos\theta$ (in contrast with the previous figures, data points in this plot corresponding to vertical and horizontal tubes are, respectively, at the right and left of the graph due to the $\cos\theta$ factor). As expected, the ratio $V_f/(V_\nu\cos\theta)$ is nearly constant in domain 3 at low $\mathrm{Re}_t\cos\theta$ values, demonstrating that $V_\nu\cos\theta$ is the proper characteristic velocity in the segregated viscous domain.

A second important feature is the excellent collapse of the data points also observed in domain 2 (in log-log coordinates they follow a straight line of slope $-1$). This results both from the additional factor $\cos\theta$ in the horizontal scale and from the fact that $\mathrm{Re}_t$ defined in Eq. (2) is identical to the ratio $V_\nu/V_t$ of the viscous and inertial characteristic velocities. The variation of the normalized velocity $V_f/(V_\nu\cos\theta)$ as $(\mathrm{Re}_t\cos\theta)^{-1}$ in Fig. 4 reduces then to the relation $V_f\propto V_t$ already demonstrated above for domain 2. Figure 4 also shows that the crossover between the viscous and the inertial regimes takes place around $\mathrm{Re}_t\cos\theta\simeq 50$. One also observes that, for larger values of $\mathrm{Re}_t\cos\theta$, the transition to the diffusive domain 1 is marked by a downwards deviation from the common trend (dashed line). It occurs for values of $\mathrm{Re}_t\cos\theta$ depending both on the density contrast At and the viscosity $\nu$, implying that this transition is determined by different scaling laws as that between domains 2 and 3.

An equivalent alternative graph placing more emphasis on the inertial regime is obtained by plotting the ratio $V_f/V_t$ as a function of the same horizontal scale $\mathrm{Re}_t\cos\theta$ (inset of Fig. 4). In this plot, domain 2 corresponds to a constant plateau value while domain 3 corresponds to a linear increase of the normalized velocity $V_f/V_t$ with $\mathrm{Re}_t\cos\theta$ (this variation is equivalent to $V_f\propto V_\nu\cos\theta$).

These experimental results allow us to separate two different flow regimes, depending on the value of $\mathrm{Re}_t\cos\theta\equiv(V_\nu/V_t)\cos\theta$. For $\mathrm{Re}_t\cos\theta\lesssim 50$, one has a stable parallel counterflow of the two fluids controlled by viscous dissipation in the whole flow volume. This flow is driven by buoyancy forces proportional to the gravity component $g\cos\theta$ along the tube and to $\Delta\rho$. For such a symmetrical counterflow, the mean velocity of each fluid is found analytically to be equal to $[1/16-1/(2\pi^2)]V_\nu\cos\theta$ assuming there is no mixing between the two liquids. Experimentally, the front velocity $V_f$ is 20% larger than this theoretical value. Note that, in this type of flow, the gravitational energy is directly dissipated by viscosity. There is no transverse mixing and, at long times, one reaches a final stable state in which the lighter fluid occupies the upper half of the tube length and the heavier one the lower half with a thin transition region.[16]

For $\mathrm{Re}_t\cos\theta\gtrsim 50$, the front velocity $V_f$ is only determined by buoyant and inertial pressure terms. From the energy conservation point of view, gravitational potential energy inputs associated to the relative motion of the two fluids are dissipated by the instabilities developed along the mixing zone. In domain 2, the front velocity has a constant value $V_f^M$ (see Fig. 3) which follows the same scaling law $V_f\propto(\mathrm{At}\,gd)^{1/2}$ as large Taylor bubbles rising into a static fluid. The factor At takes into account the finite density ratio of the two fluids and the dissipation in both fluids is neglected. This is also a similar scaling law as for internal gravity waves in thin fluid layers. This result implies that the density variation at the front is equal to the density difference $\Delta\rho$ between the

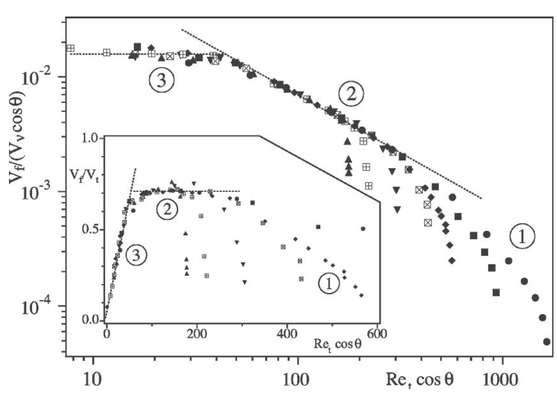


FIG. 4. Normalized front velocity $V_f/(V_\nu\cos\theta)$ dependence on weighted Reynolds number $\mathrm{Re}_t\cos\theta=V_\nu\cos\theta/V_t$ for different density contrasts and viscosities. Meanings of symbols are the same as in Figs. 2(a) and 2(b). Increasing $\mathrm{Re}_t\cos\theta$ values correspond to decreasing tilt angles $\theta$ in contrast with the previous graphs. The slope of the oblique dotted line is $-1$ (regime 2). Inset: variation of the normalized velocity $V_f/V_t$ as a function of $\mathrm{Re}_t\cos\theta$ for the same set of data points.

two fluids so that some unmixed invading fluid must reach the front. This incomplete mixing of the fluids should be related to the fact that, in this same domain 2, the concentration profile variation is not diffusive.[16]

In domain 1 (tube closer to vertical), mixing in the cross section of the tube is much more efficient while the mean concentration profile spreads diffusively. The density contrast $\delta\rho$ at the front is therefore lower than $\Delta\rho$ due to greater mixing. This reduces buoyancy forces so that one may expect that $V_f \propto (\delta\rho g/\rho)^{1/2}$ with $V_f < V_t$. The variations of the ratio $V_f/V_t$ should reflect therefore closely those of $(\delta\rho/\Delta\rho)^{1/2}$. Experimentally, one observes that $V_f/V_t$ increases in domain 1 both as the viscosity $\mu$ increases and as the Atwood number At decreases. The ratio $\delta\rho/\Delta\rho$ should therefore also increase with $\mu$ and decrease with At: this reflects the expected result that local mixing at the front will be more efficient for fluids of lower viscosity and with higher density contrasts. A similar dependence on the density contrast and the fluid viscosity was also observed in our previous work for buoyancy induced mixing in vertical tubes.[14]

To conclude, the present results demonstrate that buoyancy induced mixing in tilted tubes differs strongly from mixing in vertical tubes because of segregation due to transverse gravity components.[15] For tubes close to horizontal, these effects are so large that the two fluid flows remain totally separate. The front velocity $V_f$ is then determined by a balance between buoyancy and viscous forces *all along the tube length*. $V_f$ increases with the longitudinal gravity component (as $\theta$ decreases) until it reaches a limiting plateau value determined by a balance between inertial and buoyancy pressure terms *at the front*. The scaling law for this inertial velocity value is similar to those followed by large Taylor bubbles in tubes or by internal gravity waves in shallow fluid layers. In future work, the dependence of these scaling laws on the tube diameter will need to be investigated. For smaller tilt angles from vertical, $V_f$ is still controlled by inertial forces but is lower than the plateau value. In this latter regime, flow is weakly turbulent and the density contrast at the front (and therefore the buoyancy forces) are reduced. The scaling laws relating $V_f$ to the parameters of the flow differ from those in the two other domains: further studies of the small scale characteristics of the flow will be necessary to determine and account for them.

The authors thank C. Saurine, G. Chauvin, C. Frenois, and R. Pidoux for designing and realizing the experimental setup.

[1] M. H. I. Baird, K. Aravamudan, N. V. Rama Rao, J. Chadam, and A. P. Peirce, "Unsteady axial mixing by natural convection in vertical column," AIChE J. **38**, 1825 (1992).
[2] S. B. Dalziel, P. F. Linden, and D. L. Young, "Self-similarity and internal structure of turbulence induced by Rayleigh–Taylor instability," J. Fluid Mech. **399**, 1 (1999).
[3] G. Dimonte and M. Schneider, "Density ratio dependence of Rayleigh–Taylor mixing for sustained and impulsive acceleration histories," Phys. Fluids **12**, 304 (2000).
[4] A. W. Cook and P. E. Dimotakis, "Transition stages of Rayleigh–Taylor instability between miscible fluids," J. Fluid Mech. **443**, 69 (2001).
[5] G. Dimonte, D. L. Youngs, A. Dimits, S. Weber, M. Marinak, S. Wunsch, C. Garasi, A. Robinson, M. J. Andrews, P. Ramaprabhu, A. C. Calder, B. Fryxell, J. Biello, L. Dursi, P. MacNeice, K. Olson, P. Ricker, R. Rosner, F. Timmes, H. Tufo, Y.-N. Young, and M. Zingale, "A comparative study of the turbulent Rayleigh–Taylor instability using high-resolution three-dimensional numerical simulations: The Alpha-Group collaboration," Phys. Fluids **16**, 1668 (2004).
[6] R. M. Davies and G. I. Taylor, "The mechanics of large bubbles rising through extended fluids and through liquids in a tube," Proc. R. Soc. London, Ser. A **200**, 375 (1950).
[7] E. E. Zukoski, "The influence of viscosity, surface tension and inclination angles on the motion of long bubbles in closed tubes," J. Fluid Mech. **25**, 821 (1966).
[8] C. C. Maneri and N. Zuber, "An experimental study of plane bubbles rising at inclination," Int. J. Multiphase Flow **1**, 623 (1974).
[9] K. H. Bendiksen, "On the motion of long bubbles in vertical tubes," Int. J. Multiphase Flow **10**, 467 (1984).
[10] T. Maxworthy, "Bubble rise under an inclined plate," J. Fluid Mech. **229**, 659 (1991).
[11] J. Fabre and A. Lin, "Modelling of two-phase slug flow," Annu. Rev. Fluid Mech. **24**, 21 (1992).
[12] F. Viana, R. Pardo, R. Yanez, and J. L. Trallero, "Universal correlation for the rise velocity of Taylor bubbles in round pipes," J. Fluid Mech. **494**, 379 (2002).
[13] C. Clanet, P. Héraud, and G. Searby, "On the motion of bubbles in vertical tubes of arbitrary cross-sections: Some complements to the Dumitrescu–Taylor problem," J. Fluid Mech. **519**, 359 (2004).
[14] M. Debacq, V. Fanguet, J. P. Hulin, D. Salin, and B. Perrin, "Self-similar concentration profiles in buoyant mixing of miscible fluids in a vertical tube," Phys. Fluids **13**, 3097 (2001); M. Debacq, V. Fanguet, J. P. Hulin, D. Salin, B. Perrin, and E. J. Hinch, "Buoyant mixing of miscible fluids of varying viscosities in a vertical tube," *ibid.* **15**, 3846 (2003).
[15] G. A. Lawrence, F. K. Browand, and L. G. Redekopp, "The stability of the sheared density interface," Phys. Fluids A **3**, 2360 (1991).
[16] T. Seon, J. P. Hulin, D. Salin, B. Perrin, and E. J. Hinch, "Buoyant mixing of miscible fluids in tilted tubes," Phys. Fluids **16**, L103 (2004).
[17] A. Acrivos and E. Herbolzheimer, "Enhanced sedimentation in settling tanks with inclined walls," J. Fluid Mech. **92**, 435 (1979); E. Herbolzheimer, "Stability of the flow during sedimentation in inclined channels," Phys. Fluids **26**, 2043 (1983).
[18] T. J. Benjamin, "Gravity currents and related phenomena," J. Fluid Mech. **31**, 209 (1968).
[19] J. E. Simpson, *Gravity Currents in the Environment and the Laboratory*, 2nd ed. (Cambridge University Press, Cambridge, 1997).